

Marcin KOT\*, Jurgen LACKNER\*\*, Łukasz MAJOR\*\*\*, Marcin SZCZĘCH\*\*\*\*, Grzegorz WIĄZANIA\*\*\*\*\*, Sławomir ZIMOWSKI\*\*\*\*\*

## AN ANALYSIS OF MECHANICAL AND TRIBOLOGICAL PROPERTIES OF Zr/Zr<sub>2</sub>N MULTILAYER COATINGS

### ANALIZA WŁAŚCIWOŚCI MECHANICZNYCH I TRIBOLOGICZNYCH POWŁOK WIELOWARSTWOWYCH Zr/Zr<sub>2</sub>N

**Key words:** multilayer coatings, PVD, nanohardness, friction, wear.

**Abstract:** The paper presents the analysis of effect of the Zr to Zr<sub>2</sub>N layer thickness ratios of 1:1, 1:2, and 1:4 on the mechanical properties of Zr/Zr<sub>2</sub>N multilayer coatings. With the increase in the amount of the ceramic phase in the multilayer coating, an increase in hardness from 11 to 14.5 GPa and Young's modulus from 158 to 211 GPa was observed. This was accompanied by improved scratch resistance as critical load L<sub>c2</sub> raises from 17 to over 30 N. A ratio increase from 1:1 to 1:2 caused a 3-fold improvement in the coating wear resistance, which was also accompanied by a change in the wear mechanism. However, there was no further improvement of this parameter with a ratio increase to 1:4. Microscopic analysis of wear tracks, using the TEM technique revealed that the Zr metal layers change the direction of crack propagation. This phenomenon results in the improved fracture resistance of multilayer coatings compared to single coatings. Such a mechanism was even observed for the 1:4 coating with the thinnest 58 nm Zr layers.

**Słowa kluczowe:** powłoki wielowarstwowe, PVD, nanotwardość, tarcie, zużycie.

**Streszczenie:** W pracy przedstawiono analizę wpływu stosunku grubości warstw Zr i Zr<sub>2</sub>N 1:1, 1:2 i 1:4 na właściwości mechaniczne powłok wielowarstwowych Zr/Zr<sub>2</sub>N. Wraz ze wzrostem udziału fazy ceramicznej w powłoce wielowarstwowej obserwowano wzrost jej twardości z 11 do 14,5 GPa i modułu Younga ze 158 do 211 GPa. Towarzyszyła temu także poprawa odporności na zarysowanie, o czym świadczy wzrost wartości obciążenia krytycznego L<sub>c2</sub> z 17 do ponad 30 N. Wzrost stosunku z 1:1 do 1:2 powodował 3-krotną poprawę odporności na zużycie powłoki, czemu towarzyszyła także zmiana mechanizmu zużywania. Natomiast nie następowała dalsza poprawa tej cechy przy wzroście stosunku do 1:4. Analizy mikroskopowe torów tarcia przy użyciu techniki TEM wykazały, że warstwy metali Zr powodują zmianę kierunku propagacji pęknięć, co przekłada się na poprawę odporności na pękanie powłok wielowarstwowych w stosunku do powłok pojedynczych. Mechanizm taki obserwowano nawet dla powłoki 1:4, dla której grubość warstwy Zr była najmniejsza i wynosiła 58 nm.

\* ORCID: 0000-0002-3017-9481. University of Science and Technology, Faculty of Mechanical Engineering and Robotics, Mickiewicza 30 Ave., 30-059 Krakow, Poland, e-mail: kotmarc@agh.edu.pl.

\*\* Institute for Surface Technologies and Photonics, Functional Surfaces, Leobner Straße 94, A-8712 Niklasdorf, Austria, e-mail: juergen.lackner@joanneum.at.

\*\*\* ORCID: 0000-0002-4266-5807. Polish Academy of Sciences, Institute of Metallurgy and Materials Sciences, Reymonta 25 Street, PL-30059 Krakow, Poland, e-mail: l.major@imim.pl.

\*\*\*\* ORCID: 0000-0002-1997-357X. University of Science and Technology, Faculty of Mechanical Engineering and Robotics, Mickiewicza 30 Ave., 30-059 Krakow, Poland, e-mail: szczech@agh.edu.pl.

\*\*\*\*\* ORCID: 0000-0001-9247-0015. University of Science and Technology, Faculty of Mechanical Engineering and Robotics, Mickiewicza 30 Ave., 30-059 Krakow, Poland, e-mail: g.wiazania@gmail.com.

\*\*\*\*\* ORCID: 0000-0002-7348-8751. University of Science and Technology, Faculty of Mechanical Engineering and Robotics, Mickiewicza 30 Ave., 30-059 Krakow, Poland, e-mail: zimowski@agh.edu.pl.

## INTRODUCTION

The growing requirements for energy efficiency and durability of machines, engines, and other technical facilities demand continuous efforts to reduce the friction forces and wear of friction nodes. In tribology, two directions are developing to meet these requirements. Newer lubricants are introducing; however, they cause many problems related to the ecology of their production, collection after the operation process, and finally with their utilization. The second solution dominates where the use of oils is risky or impossible is the surface modification through various technologies in the area of surface engineering, so that the friction nodes can work in dry sliding conditions [L. 1]. Thin anti-wear coatings have been using in this field for a long time and, in recent years, mainly applied by physical techniques from the gas phase – PVD [L. 2]. The development of these technologies allowed the coatings deposition at room temperature; hence, there are no restrictions as to the extent of the material capabilities of the coating itself as well as the substrates on which the coatings can be deposited. In mechanical applications, the main problem is to protect the coating-substrate system itself against large deformations. These deformations, due to external loads, lead in a case of soft substrates, e.g., polymeric, soft metals, such as titanium alloys and soft steels, to the same deformation of the coating. On the other hand, the necessity of limiting wear causes that very hard coatings, ceramic as carbides or nitrides, of transition metals or carbon coatings, which are characterized by low resistance to cracking, are usually deposited. For such systems, large contact stresses lead to the fracture of coatings and, as a consequence, to their fragmentation which causes the wear acceleration of tribological systems when wear products remain in the friction zone.

Hence there is a strong need to produce coatings simultaneously with high hardness and with high fracture resistance. Single coatings, like TiN, CrN, TiC, and DLC cannot handle these requirements. Their hardness could be up to 40GPa, but the critical stress intensity factor  $K_{Ic}$  usually does not exceed  $5\text{MPa}\cdot\text{m}^{0.5}$  [L. 3].

The idea of a solution of this problem for engineers could be a shell where the nacre is composed of crystallites in the form of thin aragonite tablets with  $15\ \mu\text{m}$  diameters and  $0.5\ \mu\text{m}$  thicknesses. The structure also contains thin layers of organic matter not thicker than  $0.3\ \mu\text{m}$ , gluing aragonite crystallites [L. 4]. Due to this construction, the aragonite can slightly slide apart when predators are hitting the shell, without breaking the shell structure. The ceramic-metal multilayer coatings have similar structures [L. 5]. In such coatings, metal and ceramic layers with thicknesses from a few to a few hundred nanometres are arranged alternately. This causes that it is possible to obtain properties unattainable by either single metal or ceramic coatings. An appropriate selection of materials forms a structure

where thin successive layers and the typical crystalline columnar structure for PVD coatings are proportional to the thickness of these layers. This fine grained microstructure of thin layers leads to hardness increase. In addition, properly selected crystal lattices, with not too big mismatch of their parameters, give coherent or semi-coherent interlayer boundaries. Such a character of these boundaries makes them an energy barrier for dislocations motion, especially when passing from metal to ceramic layers. A large number of dislocations in metal layers at the border with ceramic ones also strengthen the metal layers. In addition, for very thin layers with a small difference in lattice parameters, an additional stress field arise due to the mismatch of the crystal lattice, while these differences cannot be too high, because the resulting interfacial boundaries are incoherent and then this mechanism stops working. The latest literature presents the results of tests for various material systems Ti/TiN [L. 6], Al/AlN [L. 7], Cr/CrN [L. 8], and others. The relations between mechanical properties of such multilayers and their period are mainly sought [L. 8, 9]. The period is the sum of the thicknesses of two successive layers, i.e. metal and ceramic. Previous works of authors allowed us to determine the optimal value of multilayer periods and to analyse the possibilities of improving crack resistance by introducing metal layers [L. 9, 10]. In this work, the research program has been undertaken to analyse the effect of the thickness ratio of metal and ceramic layers in a multilayer coating. What should be a thickness of metal to be an effective barrier for crack closing? On the other hand, thick metal layers can significantly reduce the hardness of the entire coating, and plastic deformations of the metal cause that they will no longer provide adequate support for the ceramic layers, which can easily crack. The analysis was carried out for Zr/Zr<sub>2</sub>N material system, for which coatings with different thickness ratios Zr and Zr<sub>2</sub>N were produced with the same period. Their mechanical and tribological properties were compared.

## MATERIALS AND RESEARCH METHODOLOGY

The tested Zr/Zr<sub>2</sub>N multilayer coatings along with their structure and the thicknesses of individual layers are listed in **Table 1**. They were applied by magnetron sputtering in Joanneum Research – Institute for Surface Technologies and Photonics, Niklasdorf in Austria. In order to apply multilayer coatings, the atmosphere in the chamber was changed and the mixture of nitrogen and argon gases was the Zr<sub>2</sub>N (ceramic) nitride layers, and argon was applied for Zr metal layers. The high purity Zr target was sputtered and the deposition temperature did not exceed  $40^\circ\text{C}$ . The thickness of individual layers was controlled by controlling the time of their deposition in an appropriate atmosphere, after determining the

rate of their growth for thick coatings. All coatings were deposited on X5CrNi18-10 austenitic stainless steel substrate. Steel surfaces, before deposition, were polished then degreased, washed, and placed in a vacuum chamber (Leybold Univex 450). The low roughness of the substrates, in the case of multilayer coatings,

where successive layers have small thicknesses, is very important, because, during PVD processes, the number of defects depends on substrate topography in a significant way. During the deposition, substrates were mounted on a rotating table, which provide uniformity of coatings on the whole surface.

**Table 1. Tested coatings**

Tabela 1. Badane powłoki

Coating designation	Total thickness [nm]:	Coating period $\Lambda$ [nm]	Zr layer thickness [nm]	Zr <sub>2</sub> N layer thickness [nm]
8x Zr/Zr <sub>2</sub> N r1:1	~2320	~290	~145	~145
8x Zr/Zr <sub>2</sub> N r1:2	~2370	~297	~99	~198
8x Zr/Zr <sub>2</sub> N r1:4	~2300	~288	~58	~231

Transmission electron microscopy (TEM) and Philips CM20 200 kV and JEOL EX4000 (400 kV) microscopes were used to analyse the microstructure of the coatings. Thin foils for observation were prepared using the FIB (focus ion beam) method. Nanohardness of the coatings was measured by instrumental indentation [L. 11] using NHT device manufactured by CSM Instruments. A diamond of Berkovich's geometry was used with 2 and 5 mN maximum loads. The lower load corresponded to a maximum penetration depth of up to 100 nm, i.e. below 10% of the coating thickness, which ensured that the steel substrates have no influence on the results of experiments. For each parameter, at least 6 indentations were made and the values presented are average values. Adhesion of coatings to substrates was measured using scratch tests [L. 12] using Rockwell C with 200  $\mu$ m tip radius diamond indenter. The tests were performed within 0–30 N normal load range along 5 mm scratch length. In order to precisely determine the load that caused cohesive cracks, tests were also carried out up to a load of 2 N. As a result of the tests, critical load values  $L_{c1}$  and  $L_{c2}$  were determined corresponding to the formation of the first cohesive and adhesive cracks, respectively. The analysis was based on microscopic observations of scratches after the test and an acoustic emission signal. The tribological tests were carried out in ball-on-disc geometry, using Al<sub>2</sub>O<sub>3</sub> balls,  $F = 1$  N normal load, and  $n = 20,000$  cycle number. Values of

wear index were calculated from the following relation [L. 13]:

$$W_v = \frac{V}{F \cdot l} \left[ \frac{\text{mm}^3}{\text{Nm}} \right]$$

where  $V$  – volume of removed material,  $l$  – track length.

The volume of removed material was determined from measurements of friction track profiles using a ProFilm 3D contactless profilometer (Filmetrics USA), from four places, every 90 degrees, on the circumference.

## TEST RESULTS

Microstructure observations using TEM microscopy revealed a layered structure of coatings with well separated ceramic and metal layers. **Figure 1** shows TEM images of coatings with the largest amount of the ceramic phase 1–4 ratio. Although the Zr layers have a thickness of only 58 nm, they are clearly visible on the cross-section. The structure of ceramic layers Zr<sub>2</sub>N is columnar, which is typical for ceramic coatings applied by magnetron sputtering. The observations confirmed the thickness of individual layers that were assumed at the design stage.

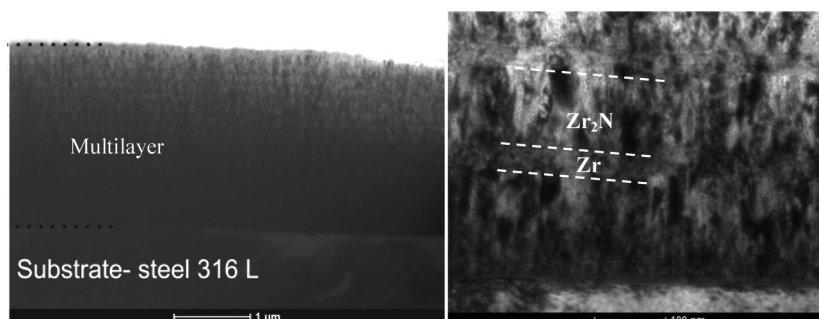


**Fig. 1. TEM images of 8x Zr/Zr<sub>2</sub>N r1:4 multilayer**

Rys. 1. Obrazy TEM powłoki wielowarstwowej 8x Zr/Zr<sub>2</sub>N r1:4

The results of indentation tests (nanohardness and elasticity modulus) are presented in **Fig. 2a** and **2b**, respectively. Experiments showed that the nanohardness increases with increasing the thickness of the ceramic layers from 11 to 14.5 GPa (**Fig. 2a**). The values measured for the 5 mN load are about 10% smaller, which is probably related to the fact that deformation reaches the substrate with significantly lower hardness  $H = 2.5$  GPa than the coating. A similar relationship was found for elasticity modulus (**Fig. 2b**) and its increase from 158 to 211 GPa. In both figures, the values calculated from rule of mixtures (RM) were added from tests which were performed previously for 1  $\mu\text{m}$  thick single coatings, for which the hardness and elasticity

modulus are  $H = 5$  and 16 GPa,  $E = 120$  and 220 GPa for Zr, and  $\text{Zr}_2\text{N}$ , respectively. The biggest differences between predicted values from RM and experimental results were found for the coating with the highest amount of ceramic phase. This may be due to the finest microstructure of metallic layers with a thickness of 58nm, which can significantly increase the hardness compared to the same single Zr coating, but thicker. Of course, ceramic coatings also have a smaller thickness, whereas, in multilayer coatings, it increases with rising ratio of the ceramic phase to r1-4. Interfaces between layers that restricts movement of dislocations and plastic deformation also play some effect, but in all tested multilayers, their number is the same.

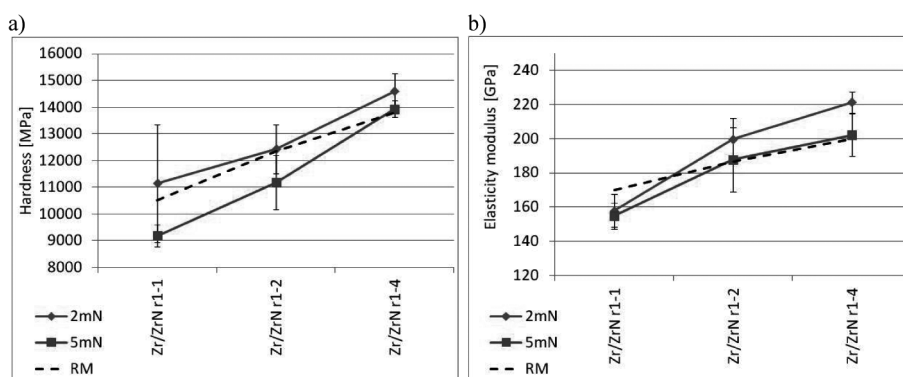


**Fig. 2. Indentation test results: a) nanohardness, b) elasticity modulus**

Rys. 2. Wyniki testów indentacyjnych: a) nanotwardość, b) moduł sprężystości

An extremely important parameter for the coating-substrate systems, deciding the ability to transfer contact loads, is their fracture resistance and the strength of coating to substrate interface. For  $8x\text{Zr}/\text{Zr}_2\text{N}$  r1-1 multilayer, with the largest amount of a soft and pliable metallic phase, the first small cracks could be seen at low 0.9 N load (**Fig. 3a**), which is due to the low stiffness of the coating. However, they are not particularly dangerous, because microcracks probably appear only in outer  $\text{Zr}_2\text{N}$  layer. Concave cracks indicate that they were caused by tensile stress behind the indenter. The load increase up to 17.5 N induced coating removals and a small area of substrate exposure (**Fig. 3b**).

The removal of buckled parts due to compressive stress from the whole scratch width occurred at a load of 26.6 N. The remaining, attached coating fragments are highly cracked, and the substrate is visible at the bottom of the groove. Whereas, for the  $8x\text{Zr}/\text{Zr}_2\text{N}$  r1-2 multilayer, the first coarse cracks of  $\text{Zr}_2\text{N}$  top layer were formed behind indenter at 1.7 N load (**Fig. 4a**). The change in their character and size took place at 19.5 N (**Fig. 4b**), when the cracks are caused by compressive stresses in front of the indenter. The

coating with a 1:2 ratio has a much better adhesion to the substrate than the coating with a 1:1 ratio. The coating was not delaminated, but removed from the substrate due to abrasion at the load  $L_{C2} = 28.4$  N (**Fig. 4c**).

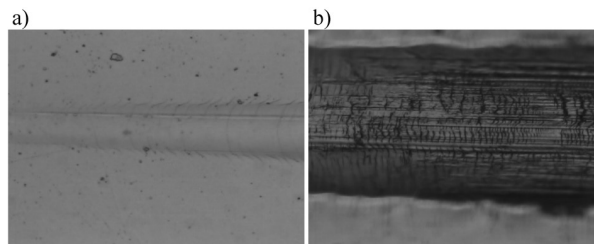


**Fig. 3. Images of scratches of  $\text{Zr}/\text{Zr}_2\text{N}$  r1-1 coating at characteristic loads: a) 0.9 N, and b) 17.5 N**

Rys. 3. Obrazy toru zarysowania powłoki  $\text{Zr}/\text{Zr}_2\text{N}$  r1-1 przy obciążeniach charakterystycznych: a) 0,9 N, b) 17,5 N

Thus, the increase in amount of ceramic phase from r1-1 to r1-2 causes an increase in the critical loads.  $L_{C1}$  and  $L_{C2}$  critical loads for all coatings are listed in **Table 2**. For the  $8x\text{Zr}/\text{Zr}_2\text{N}$  r1-4 multilayer, the cohesive

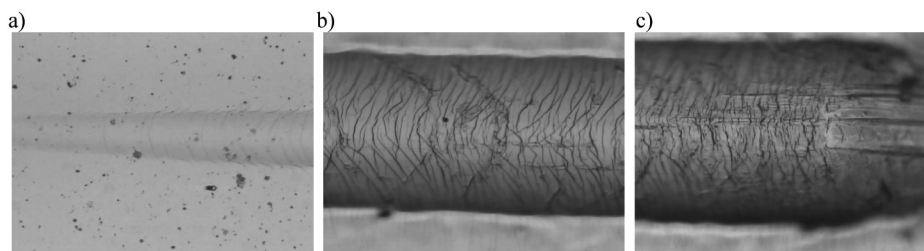


**Fig. 4. Images of scratches of Zr/Zr<sub>2</sub>N r1-2 coating at characteristic loads: a) 1.7 N, b) 19.5 N, and c) 28.4 N**

Rys. 4. Obrazy toru zarysowania powłoki Zr/Zr<sub>2</sub>N r1-2 przy obciążeniach charakterystycznych: a) 1,7 N, b) 19,5 N, c) 28,4 N

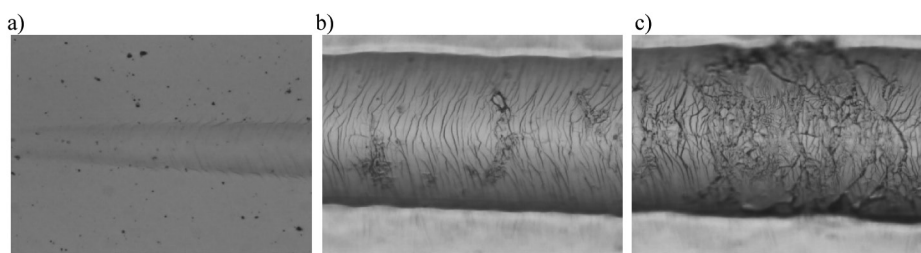


**Fig. 5. Images of scratches of Zr/Zr<sub>2</sub>N r1-4 coating at characteristic loads: a) 1 N, b) 18.8 N, and c) 23.3 N**

Rys. 5. Obrazy toru zarysowania powłoki Zr/Zr<sub>2</sub>N r1-4 przy obciążeniach charakterystycznych: a) 1 N, b) 18,8 N, c) 23,3 N

cracks (**Fig. 5a**) appeared at loads of 1N and 18.8 N caused the formation of bigger conformal cracks (**Fig. 5b**). This coating, like coating with 1:2 ratio, is covered with a network of cracks caused by compression and tension before and after the indenter, while the number of cracks due to compressive stress seemed to be smaller. At 23.3 N, the top layer is removed; however, the substrate is not exposed. The maximum load of 30 N does not completely destroy the coating; therefore,  $Lc_2 > 30$  N is entered in **Table 2**.

**Table 2. Critical load values of Zr/Zr<sub>2</sub>N multilayers**

Tabela 2. Wartości obciążeń krytycznych powłok wielowarstwowych Zr/Zr<sub>2</sub>N

Coating	$Lc_1$	$Lc_2$
8x Zr/Zr <sub>2</sub> N r1-1	0.9±0.3 N	17.5±1.5 N
8x Zr/Zr <sub>2</sub> N r1-2	1.7±0.5 N	28.4±2.3 N
8x Zr/Zr <sub>2</sub> N r1-4	1±0.3 N	>30 N

The tribological tests showed that the 8xZr/Zr<sub>2</sub>N r1-1 coating is characterized by the largest wear from all tested coatings. It was about three times larger than the other multilayer coatings. Probably, the low stiffness of the coating, its low hardness, and the occurrence of large plastic deformations observed in scratch tests led to high wear. These plastic deformations of Zr layers increase the deformation of the coating, causing the fracture of Zr<sub>2</sub>N ceramics layers and the removal of coating fragments at cyclically repeated contact. **Figure 6a** shows longitudinal grooves in wear track, which may also indicate that wear products remain in the friction zone intensifying the abrasive wear process.

It is also visible in images of the ball at the magnification of 200x, where the fragments of the ceramic having a golden colour are recessed in the surface of the sphere (**Fig. 6d**). The 8xZr/Zr<sub>2</sub>N r1-2 coating exhibited the best wear resistance among all samples coated with multilayers. The sample profiles were characterized by the occurrence of relatively small

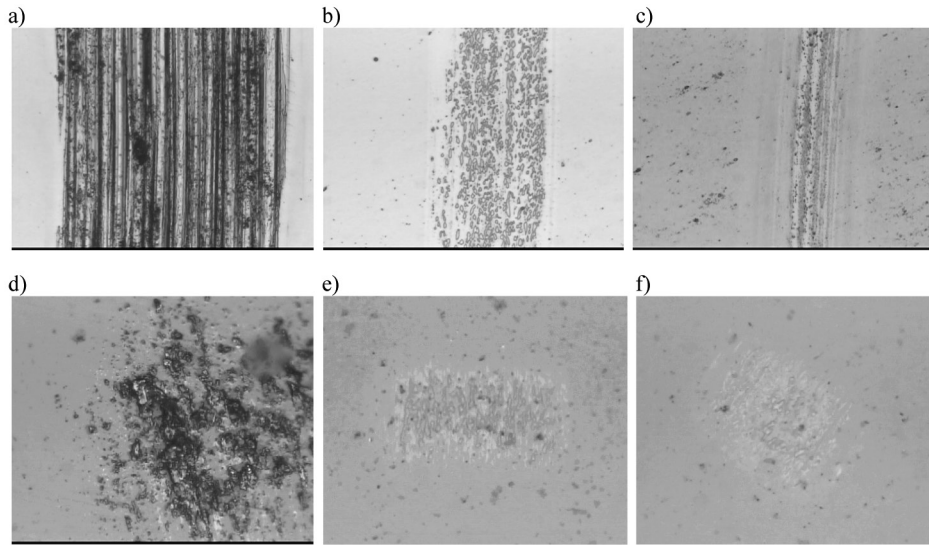
**Table 3. Summary of tribological test results of tested coatings**

Tabela 3. Zestawienie wyników testów tribologicznych badanych powłok

Coating	Furrow section area [mm <sup>2</sup> ]	Volume of material removed [mm <sup>3</sup> ]	Wear indicatory W [mm <sup>3</sup> /N*m]	Coefficient of friction
8x Zr/Zr <sub>2</sub> N r1-1	31.1·10 <sup>-6</sup>	5.9·10 <sup>-4</sup>	15.5±2.7 ·10 <sup>-6</sup>	0.15
8x Zr/Zr <sub>2</sub> N r1-2	10.2·10 <sup>-6</sup>	1.9·10 <sup>-4</sup>	5.1±1.9 ·10 <sup>-6</sup>	0.1
8x Zr/Zr <sub>2</sub> N r1-4	13.5·10 <sup>-6</sup>	2.5·10 <sup>-4</sup>	6.7±1.6 ·10 <sup>-6</sup>	0.1

pile-ups, and the maximum groove depth was about  $0.4 \mu\text{m}$ , so the coating was not completely rubbed off (**Fig. 6b**). The size of wear area on the ceramic ball indicates its low wear and the absence of detached large coating fragments in the contact zone (**Fig. 6e**). The last of the tested coatings,  $8x\text{Zr}/\text{Zr}_2\text{N}$  r1-4, has only slightly

worse wear resistance than the coating with r1-2, and images of the wear track and the surface of the ball indicate a similar nature of wear to the  $8x\text{Zr}/\text{Zr}_2\text{N}$  r1-2 coating. The average values of the coefficient of friction 0.1–0.15 are similar for all tested samples (**Table 3**).



**Fig. 6. Wear track images of coatings: a)  $8x\text{Zr}/\text{Zr}_2\text{N}$  r1-1, b)  $8x\text{Zr}/\text{Zr}_2\text{N}$  r1-2, c)  $8x\text{Zr}/\text{Zr}_2\text{N}$  r1-4, and balls after tribological tests: d)  $8x\text{Zr}/\text{Zr}_2\text{N}$  r1-1, e)  $8x\text{Zr}/\text{Zr}_2\text{N}$  r1-2, and f)  $8x\text{Zr}/\text{Zr}_2\text{N}$  r1-4**

Rys. 6. Obrazy torów tarcia powłok: a)  $8x\text{Zr}/\text{Zr}_2\text{N}$  r1-1, b)  $8x\text{Zr}/\text{Zr}_2\text{N}$  r1-2, c)  $8x\text{Zr}/\text{Zr}_2\text{N}$  r1-4 oraz kul po testach tribologicznych: d)  $8x\text{Zr}/\text{Zr}_2\text{N}$  r1-1, e)  $8x\text{Zr}/\text{Zr}_2\text{N}$  r1-2, f)  $8x\text{Zr}/\text{Zr}_2\text{N}$  r1-4

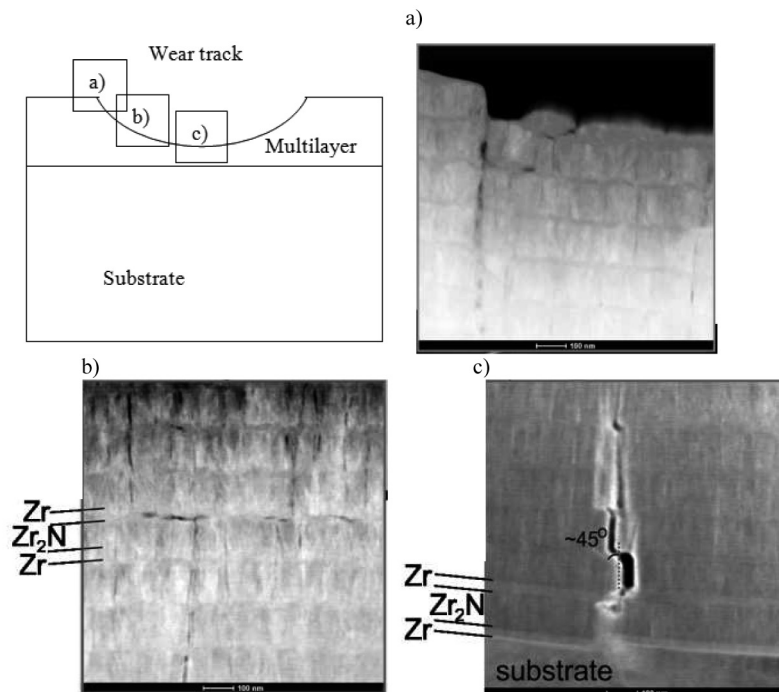


**Fig. 7. TEM images of wear track of  $8x\text{Zr}/\text{Zr}_2\text{N}$  r1-4 in areas pointed on the scheme and designated a), b), and c)**

Rys. 7. Obrazy TEM toru tarcia powłoki  $8x\text{Zr}/\text{Zr}_2\text{N}$  r1-4 w obszarach zaznaczonych na schemacie oznaczonych a), b) i c)

A slightly higher value for  $8xZr/Zr_2N$  r1-1 coating is probably due to the presence of wear products in the friction zone. TEM images of the wear track of  $8xZr/Zr_2N$  r1-4 coating are shown in **Fig. 7**. Thin foils were made in three characteristic places marked on the schematic drawing of the wear track. In the area (a), i.e. the nearest to edge of track, cracks appear on the surface of the coating and propagate perpendicularly to the coating surface. They result from a high concentration of tensile stresses on the surface in this area. These observations confirm numerical analyses carried out using the finite element method and presented in a previous paper [**L. 14**].

These cracks are stopped on Zr metal layers after passing one or just a few ceramic layers. Each of the metal layers caused that the increase in the load is necessary to induce crack initiation in the next ceramic layer.

FEM analyses show that it may be the multiple raise of critical load destroying the multilayer coating in relation to a single thick ceramic coating [**L. 14**]. For the area closer to the centre of the wear track (Area b), cracks are formed closer to middle of coating thickness, but they do not propagate completely towards the surface or towards the coating-substrate interface. In the last analysed area (c), the cracks start near the substrate and propagate towards the surface, but, similarly as in the previous cases, they are smaller and smaller on subsequent ceramic layers.

## CONCLUSIONS

Multilayer coatings consisting of alternate metal and ceramics layers are increasingly being developed. An appropriate choice of the thickness of these layers can

be crucial, considering their mechanical and tribological properties. Results presented in this paper have shown that  $Zr/Zr_2N$  coatings with an increased amount of ceramic phase have significantly better properties than  $Zr/Zr_2N$  coating with the same thicknesses of Zr and  $Zr_2N$  layers. The hardness of  $8xZr/Zr_2N$  r1-4 coating  $H = 14.5$  GPa is 30% higher than for  $8xZr / Zr_2N$  r1-1 coating. In spite of its higher stiffness, the greater value of the elasticity modulus, it exhibited greater scratch resistance. The critical load value is above 30N, while, for  $8xZr/Zr_2N$  r1-1,  $L_{C2} = 17.5$  N. Moreover, both coatings with increased thicknesses of  $Zr_2N$  layers are characterized by a 2.5–3 times higher wear resistance. These results indicate that, in multilayer ceramics/metal coatings, ceramic layers should be thicker than metal ones. The 60 nm thickness of Zr layers is sufficient to effectively block the cracks formed in the ceramic layers. Too thick metal layers result in a lower hardness of the coatings and facilitate deformations due to their plasticity. A further process of testing of such systems is planned with coatings deposition with an even greater contribution of the ceramic phase, e.g., 1–8. However, as shown in literature studies, this may lead to the loss of the multilayer structure of coatings and the deterioration of their properties [**L. 4, 8**].

## ACKNOWLEDGEMENTS

The work was carried out as part of research conducted at the AGH University of Science and Technology in Krakow at the Faculty of Mechanical Engineering and Robotics, subsidy 16.16.130.942.

## REFERENCES

1. Holmberg K., Matthews A.: Coatings Tribology, Second Edition. Oxford, Elsevier, 2009.
2. Zhao L.R., Chen K., Yang Q., Rodgers J.R., Chiou S.H.: Materials informatics for the design of novel coatings. *Surface and Coatings Technology*, 200 (2005), pp. 1595–1599.
3. Zhang S., Sun D., Fu Y., Du H.: Toughness measurement of thin films: a critical review. *Surface and Coatings Technology*, 198 (2005), pp. 74–84.
4. Lackner J.M., Waldhauser W., Major B., Major L., Kot M.: Plastic deformation in nano-scale multilayer materials – a biomimetic approach based on nacre. *Thin Solid Films*, 534 (2013), pp. 417–425.
5. Kot M., Major Ł., Lackner J., Rakowski W.: Badanie odporności na pękanie i zużycie przez tarcie powłok wielowarstwowych. *Tribologia*, 254 (2014), pp. 89–99.
6. Lackner J.M., Major Ł., Kot M.: Microscale interpretation of tribological phenomena in Ti-TiN soft-hard multilayer coatings on soft austenite steel substrates. *Biulletin of Polish Academy of Sciences. Technical Sciences*, 59/3 (2011), pp. 343–355.
7. Wu Z.G., Zhang G.A., Wang M.X., Fan X.Y., Yan P.X., Xu T.: Structure and mechanical properties of Al/AlN multilayer with different AlN layer thickness. *Applied Surface Science*, 253 (2006), pp. 2733–2738.
8. Romero J., Esteve J., Lousa A.: Period dependence of hardness and microstructure on nanometric Cr/CrN multilayers. *Surface and Coatings Technology*, 188–189 (2004), pp. 338–343.

9. Kot M., Major L., Lackner J., Rakowski W.: Enhancement of mechanical and tribological properties of Ti/TiN multilayers over TiN single layer, *Journal of the Balkan Tribological Association*, 18 (2012), pp. 92–105.
10. Kot M., Rakowski W., Zimowski S.: Efekt synergiczny w multiwarstwach typu Ti/TiN oraz Cr/CrN w świetle badań mikromechanicznych i tribologicznych. *Tribologia*, 218 (2008), pp. 297–307.
11. ISO 14577-1:2015 Metallic materials – instrumented indentation test for hardness and material parameters – Part 1: Test method.
12. EN 200502:2005. Advanced technical ceramics – methods of test for ceramic coatings – Part 3: determination of adhesion and other mechanical failure modes by a scratch test.
13. ISO 20808:2016. Fine ceramics (advanced ceramics, advanced technical ceramics) – determination of friction and wear characteristics of monolithic ceramics by ball-on-disc method.
14. Kot M.: Contact mechanics of coating-substrate systems: single and multilayer coatings. *Archives of Civil and Mechanical Engineering*, 12 (2012), pp. 464–470.